Field Effect and Strongly Localized Carriers in the Metal-Insulator Transition Material VO_2

K. Martens,[1,2,3] J. W. Jeong,[1] N. Aetukuri,[1] C. Rettner,[1] N. Shukla,[6] E. Freeman,[6] D. N. Esfahani,[4] F. M. Peeters,[4] T. Topuria,[1] P. M. Rice,[1] A. Volodin,[5] B. Douhard,[3] W. Vandervorst,[3,5] M. G. Samant,[1] S. Datta,[6] and S. S. P. Parkin[1]
[1]IBM Research-Almaden, San Jose, California 95120, USA
[2]ESAT Department, KU Leuven, Leuven BE-3001, Belgium
[3]IMEC, Kapeldreef 75, Leuven BE-3001, Belgium
[4]Physics Department, University of Antwerp, Groenenborgerlaan 171 BE-2020, Antwerp BE-2020, Belgium
[5]Department of Physics and Astronomy, KU Leuven, Leuven BE-3001, Belgium
[6]Department of Electrical Engineering, Pennsylvania State University, University Park, Pennsylvania 16802, USA
(Received 19 January 2015; published 4 November 2015)

The intrinsic field effect, the change in surface conductance with an applied transverse electric field, of prototypal strongly correlated VO_2 has remained elusive. Here we report its measurement enabled by epitaxial VO_2 and atomic layer deposited high-κ dielectrics. Oxygen migration, joule heating, and the linked field-induced phase transition are precluded. The field effect can be understood in terms of field-induced carriers with densities up to $\sim 5 \times 10^{13}\ \mathrm{cm}^{-2}$ which are strongly localized, as shown by their low, thermally activated mobility ($\sim 1 \times 10^{-3}\ \mathrm{cm}^2/\mathrm{V\,s}$ at 300 K). These carriers show behavior consistent with that of Holstein polarons and strongly impact the (opto)electronics of VO_2.

DOI: 10.1103/PhysRevLett.115.196401 PACS numbers: 71.30.+h, 71.27.+a, 71.38.-k, 85.30.Tv

VO_2 is a prototypical material with strong electron-electron and electron-phonon interactions and with a sharp thermally driven metal-insulator transition (MIT) near room temperature. Below T_{MIT}, VO_2 has a monoclinic crystal structure (M_1) with dimerized V atoms and a $\sim$0.6 eV band gap [1], while above T_{MIT} it is metallic with a rutile structure. In recent work [1–3], VO_2 below its transition temperature is not considered a pure Mott insulator but a many-body Peierls insulator with combined influences of electron correlations and Peierls effects. A more complete understanding of VO_2's first-order phase transition is currently being pursued [4–6].

Interest has been raised in the electric field effect in highly correlated materials due to the possibility of a direct electrostatically induced metal-insulator transition, enabling a Mott transistor [7–9]. Such Mott transistor behavior has not been rigorously proven in correlated oxides [9]. Recently, ionic liquid gating experiments showed that semiconducting VO_2 can be rendered metallic by applying an electric field normal to VO_2's interface [9]. However, Jeong *et al.* [10] showed that oxygen migration occurs during ionic liquid gating. At present the nature of the VO_2 field effect without oxygen migration remains an open question. The basic understanding of the VO_2 field effect in field ranges used in typical silicon field effect transistors is the focus of this work.

The intrinsic effect of a transverse electric field on surface conductance (field effect) in VO_2, one of the simplest strongly correlated oxides, remains to be measured and understood. To measure the intrinsic VO_2 field effect we exclude the presence of oxygen migration, found using ionic liquid gating, by applying transverse electric fields using a solid gate dielectric. We have probed the intrinsic field effect in VO_2 by making use of ultrathin (<10 nm) single crystalline VO_2 films. These avoid large unmodulated "bulk" conduction which has made measuring the small VO_2 field effect problematic. We evaluated the field effect in a wide range of field-induced excess charge densities. The maximum density is limited by dielectric breakdown, and at the obtained densities field-induced MITs have been reported using ionic liquid gating.

The existence of strongly localized carriers intrinsic to VO_2 has been discussed by, e.g., Zylbersztejn and Mott [11] and Goodenough [12] and is often assumed [9,13]. Experimental evidence of strongly localized carriers in VO_2 [14,15] is based on magnetic resonance and susceptibility measurements in incompletely dimerized M_2 VO_2. Based on Hall measurements [16], carriers in VO_2 are often considered to behave as band carriers on the verge of localization rather than strongly localized carriers. However, Hall density and mobility are only interpreted correctly as the actual carrier density and mobility when rightly assuming band transport, which is not known to be correct for VO_2 [16]. VO_2 carrier mobility from field effect measurements has not been reported and our measurements provide evidence for the existence of strongly localized carriers intrinsic to VO_2.

To reliably assess the gate field effect with field-induced charge densities similar to those obtained with ionic liquid gating ($\sim 5 \times 10^{13}\ \mathrm{cm}^{-2}$), we fabricated VO_2 field effect transistor structures (FETs) [see inset Fig. 1(b)] with single crystalline VO_2 films 3–10 nm thin and high-κ dielectrics. Single crystalline VO_2 allows an assessment of properties unaffected by grain boundaries. High-quality high-κ dielectrics allow sustaining high charge densities at high fields without leading to oxide degradation and increased gate leakage. Little work was done on the VO_2 field effect making use of solid dielectrics [17–19], and the work done made use

 © 2015 American Physical Society

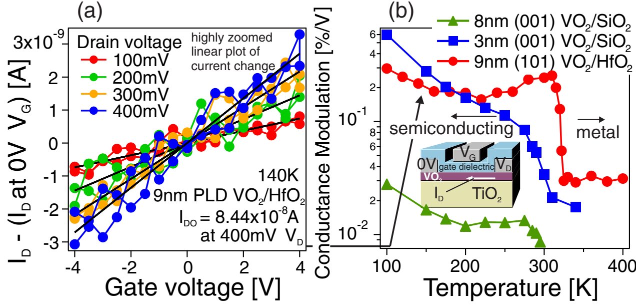

FIG. 1 (color online). (a) Gate modulation of drain current (I_D). Zoomed linear plot of ΔI_D relative to I_D at 0 V gate bias (I_{D0}) for 9 nm PLD $VO_2(101)/HfO_2$, $L = 7\ \mu m$ and $W = 80\ \mu m$. Up and down voltage sweeps are shown. (b) Field effect modulation of drain current [%/V] expressed as $d(\Delta I_D/I_{D0})/dV_G$.

of polycrystalline thick VO_2 (~100 nm) with dielectrics with low permittivity (κ) which are susceptible to dielectric degradation. Careful gate current monitoring throughout our experiments excludes dielectric degradation effects. Any switching reported in previous work is either induced by applying a significant lateral field besides a normal gate field [18] or the switching occurs slowly (seconds to minutes) excluding a direct electronic or intrinsic VO_2 cause [17]. All measurements in this work use low lateral fields (20–500 mV drain-to-source bias) to avoid joule heating and to focus on the transverse field effect. Previously, electric field driven metallization in lateral 2-terminal VO_2 devices was explained by joule heating [20–23].

Devices were fabricated in three different labs making use of films deposited with multiple techniques. Epitaxial single crystal VO_2 films were grown by pulsed laser deposition (PLD) at 400 °C and in 10 mtorr O_2 using a VO_2 target [20,24,25] on TiO_2 (001) or (101) substrate. The tensile strained VO_2 films on TiO_2 have a lower T_{MIT} as compared to the bulk [24]. XRD and TEM show that the films are monocrystalline (see Ref. [26] for details). The 3 nm PLD VO_2 films are capped with 0.7 nm thick PLD TiO_2 to avoid degradation of the MIT [39]. 10 nm thick VO_2 films were epitaxially grown on TiO_2 (001) employing reactive oxide MBE [26,40] as well.

FETs were fabricated with gate dielectrics that were deposited by either ion beam deposition of 15 nm thick SiO_2 at room temperature on VO_2/TiO_2 (001) or by atomic layer deposition (ALD) at 200 °C using water and $HfCl_4$ [41] of 10 nm thick HfO_2 on VO_2/TiO_2 (101). Fabrication made use of electron beam lithography and gate lengths were 6–9 μm. The magnitude of conductance change at T_{MIT} for the VO_2 channels in patterned devices is comparable to that in blanket films indicative of no significant degradation of VO_2 during device fabrication [26]. The MBE VO_2 devices have a 1 nm thick Al_2O_3 gate dielectric with a 7 nm thick HfO_2 deposited on top by ALD at 100 °C and 110 °C, respectively (see Ref. [26]).

Capacitance measurements require low series resistance; hence, dedicated capacitors were fabricated with 8 nm thick VO_2 films grown epitaxially on a conducting 5 nm thick sputtered RuO_2 layer grown epitaxially on TiO_2 (001) [26]. The dielectric was either a 32 nm thick SiO_2 or a 10 nm thick HfO_2 layer. For each VO_2/dielectric stack the capacitors were fabricated using the same process as the FETs.

For the HfO_2 dielectric, the estimated charge density induced by the gate voltage in the VO_2 channel reached a maximum of $5 \times 10^{13}\ cm^{-2}$ (from $C'_{di} \times V_G/e$, where V_G is the gate voltage and C'_{di} is dielectric capacitance). The corresponding maximum field reached ~4 MV/cm for HfO_2 (assuming relative permittivity $\varepsilon_{rVO_2} = \sim 30$ [42], $\varepsilon_{rHfO_2} = 20$, $V_G = \pm 6$ V) and 0.2 MV/cm for SiO_2 ($\varepsilon_{rSiO_2} = 3.9$, $V_G = \pm 3.4$ V). These fields are near the maximum that can be sustained without compromising dielectric reliability. Ionic liquid gating can result in metallization well below a $\sim 5 \times 10^{13}\ cm^{-2}$ capacitively induced charge density [9] (see Fig. 4 in the Supplemental Material [26]). Given the different nature of liquid and solid gating, the presence of any field-induced MIT is not expected to occur at similar electric field.

A field effect measurement is shown in Fig. 1(a) for a $(101)VO_2/HfO_2$ sample as the change in channel or drain current with V_G. The drain current of all the evaluated device types shows a small and approximately linear dependence on V_G over a large field and temperature range (80–400 K). For more characteristics, see Ref. [26]. Gate modulation (%/V) of conductance or drain current is defined here as $(dI_D/dV_G)/I_{D0}$, $I_{D0} = I_D(V_G = 0\ V)$ and is shown in Fig. 1(b). Gate modulation is derived by linear fitting [Figs. 1(a) and 1(b)] and does not vary strongly with temperature, in contrast to channel resistivity. Drain currents are modulated by less than 0.6%/V by field effect gating [Fig. 1(b)] [26]. Because of the lack of any concomitant electrochemical or joule heating process in the FET devices, previously observed field-induced MITs are absent [9] at any of the measurement temperatures above or below the MIT (80–400 K) in any of the devices, independent of gate dielectric, VO_2 thickness, VO_2 growth method, and crystallographic orientation.

We obtain the mobility μ_{FE} of the excess carriers induced by the field at the interface [Fig. 2(a)] as $\mu_{FE} = \sigma/(C_{di}V_G)$, where conductivity $\sigma = L/W \bullet \Delta I_D/V_D$, with $\Delta I_D = I(V_G) - I(0\ V)$. W is gate width and L is gate length. μ_{FE} (Fig. 2) is significantly smaller than a critical mobility $2a^2e/\hbar = 0.4\ cm^2/V\,s$ below which charge carrier localization is estimated to occur when the mean free path is shorter than the nearest-neighbor distance $a = 0.3$ nm [43]. The excess carrier mobility shows temperature activation, a hallmark of charge carrier localization. The low mobility of the field-induced excess charge explains the magnitude of the VO_2 field effect conductance modulation.

The most straightforward potential explanations for the observed strongly subdued gate field effect are evaluated: conventional semiconductor behavior, a very high density of defects which inhibit field effect modulation, electron-electron correlation effects, the formation of small

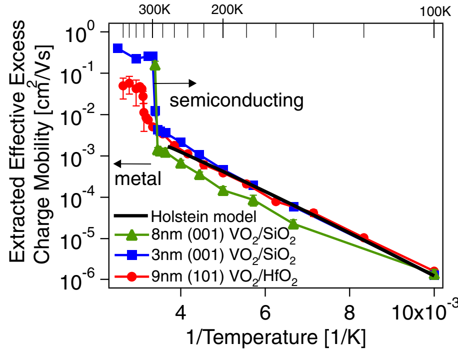

FIG. 2 (color online). Extracted excess charge field effect mobility and fit of Holstein small polaron model.

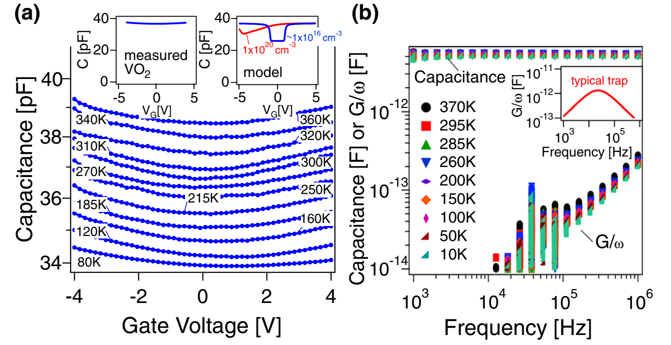

FIG. 3 (color online). (a) C-V's at 100 kHz for a 10 nm $HfO_2/VO_2(001)$ capacitor. Right-hand inset shows conventional semiconductor model for 1×10^{20} cm^{-3} doping at 300 K and 1×10^{16} cm^{-3} doping at 100 K. (b) Conductance-frequency [G plotted normalized by $2\pi f=\omega$, 30 mV ac bias) characteristics of $SiO_2/TiO_2/VO_2(001)/RuO_2$ capacitors]. Inset is the expected G/ω conventional semiconductor trap signature for defects.

polarons, of which the presence is anticipated due to the strong electron-phonon interactions in VO_2 [44,45], and disorder.

If VO_2 were to behave as a conventional band semiconductor, one would observe a large field effect. In such a hypothetical scenario, the Hall mobility of ~0.5 $cm^2/V\,s$ [16,46] approximately reflects the actual carrier mobility. Using the carrier density derived from Hall measurements, the amount of carriers in a 10 nm thick VO_2 channel ($<\sim1\times10^{19}$ cm^{-3} or $<\sim1\times10^{13}$ cm^{-2}) would be smaller than what can be induced by the gate (5×10^{13} cm^{-2}). The channel could then easily be fully depleted of carriers by the field, and the current could be pinched off completely. Such conventional semiconductor behavior is clearly not present.

Figure 4a presents the schematics of band bending and mobile carrier modulation in conventional semiconductors for a gate bias corresponding to carrier accumulation (a1 and a3) and depletion (a2 and a4) [47]. In depletion, mobile carriers are removed from the semiconductor volume [a4 in Fig. 4(a)], whereas in accumulation they are added at the dielectric-channel interface [a3 in Fig. 4(a)]. If carriers were depleted throughout a significant fraction of the VO_2 film depth by gating, a significant change in channel current would result. The absence of field effect current modulation entails the absence of significant depletion of carriers in the volume of VO_2. This points to field-induced net (excess) charge formation at the VO_2-dielectric interface.

We corroborate the absence of conventional semiconductor depletion behavior and the presence of excess charge at the interface with capacitance (C) measurements. The ac capacitance (Fig. 9(a,c) in [26]) shows no abrupt change versus temperature at the MIT at all gate voltages (V). Hence, the location of the ac modulated excess charge is near the dielectric-VO_2 interface in both the metallic and semiconducting phases. In a conventional semiconductor, depletion gives rise to a characteristic drop in the C-V characteristic [Fig. 3(a), right-hand inset] due to the location of ac modulated charge at the depletion edge, away from the interface [a4 in Fig. 4(a)]. This typical drop is observed to be absent in the VO_2 C-V [Fig. 3(a)] across all temperatures. For the HfO_2 capacitors, a 40% capacitance drop [26] would be expected for conventional semiconductor behavior when fully depleting VO_2. For all temperatures the small change ($<2\%$) in C-V shows a parabolic voltage dependence (see Ref. [26]), typical for metal-insulator-metal capacitors [48,49].

Defects were investigated as a potential determining factor of the field effect. It is well known in field effect devices with conventional semiconductors (e.g., GaAs) that field effect conductivity modulation can be suppressed by the presence of a large number of interface trap defects, which immobilize the excess charge carriers. The presence of such interface traps results in a peak in capacitor conductance (G/ω) spectroscopy measurements [inset Fig. 3(b)], with the G/ω peak intensity versus ω proportional to the density of traps [50]. The inset of Fig. 9(c) in Ref. [26] shows a schematic of a measured capacitor. A G/ω peak is not observed in capacitors [Fig. 3(b)] [26] for any of the dielectric-VO_2 combinations studied over the entire temperature range (10 K, 80–400 K). This temperature range ensures that interface traps, if present, would have been detected as we covered all likely capture cross sections and band gap energy levels [51]. The observed monotonic slope in G/ω versus ω is due to the series resistance of the RuO_2 backplane, which was low by design to enable interface trap evaluation. No signature of interface traps was found.

Moreover, for defect-related types of hopping transport a frequency (f) dependence of the ac channel conductance of ($\propto f^s s\sim0.8$) is expected [52], which is not observed in the VO_2 devices [26]. Scenarios involving a high dopant density or bulk defects require a very large amount of defects to explain the strongly subdued field effect [e.g., exceeding $(4–10)\times10^{21}$ cm^{-3}, $\sim10\%$ of V atom density [26]] and should be easily observable. In scanning tunneling microscopy measurements [Fig. 4(b)] [26], no such large density of states within VO_2's gap was found. We find a defect-dominated scenario to be unlikely.

To assess whether strong electron-electron interactions could explain the field effect and absence of depletion for

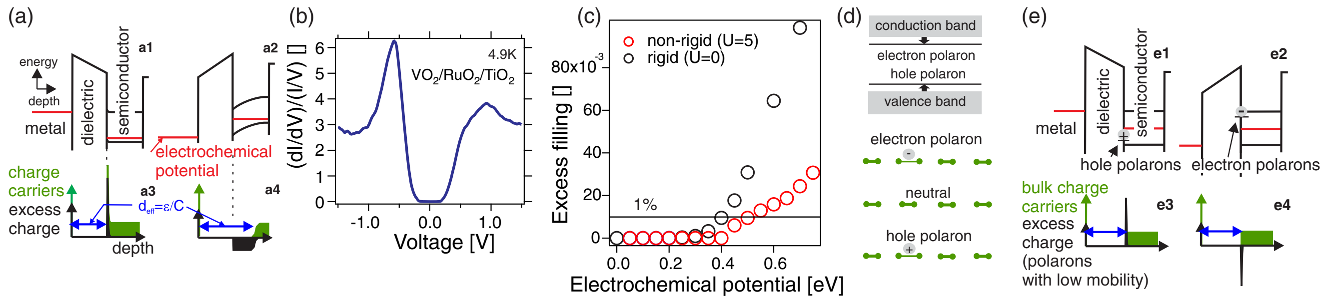

FIG. 4 (color online). (a) Band (a1 and a2) and charge (a3 and a4) diagrams of a classical semiconductor in accumulation (a1 and a3) and depletion (a2 and a4). Net, excess charge (black) and mobile carriers (green) (b) STM of VO_2 on RuO_2 (c) Excess filling (difference with half filling) versus electrochemical potential shift (shift compared to charge neutral condition) from the correlated-band insulator Hubbard model for the correlated ($U = 5$) and the uncorrelated ($U = 0$) case. (d) Band diagram and dimer chain illustration of polaron formation. (e) Band and charge diagrams in case small polarons form.

VO_2, we have calculated the volume excess charge (Δn) versus electrochemical potential shift ($\Delta\mu$) relationship, which determines the presence of depletion [47]. A Hubbard model appropriate to address a dimerized correlated-band insulator or many-body Peierls phase [2,3] like VO_2 was solved using dynamic mean-field theory (DMFT) [53]. The Hamiltonian was adapted from Ref. [54]. See Ref. [26] for details. We choose $t = 1$ eV (interdimer hopping) and $t' = 0.5$ eV (intradimer hopping) resulting in a gap similar to the gap of VO_2. U, the on-site Coulomb repulsion, was chosen 0 and 5 eV and the inverse of temperature is fixed to $\beta = (30/t)$. Strong correlations ($U > 0$) are not found to result in an excess charge >1% for small $\Delta\mu$, similar to that in the uncorrelated, conventional semiconductor case ($U = 0$); see Fig. 4(c). 1% is the approximate amount of filling (compared to V atom density) corresponding to accumulating $\sim 5 \times 10^{13}$ cm^{-2} of carriers in 1 nm of VO_2. Depletion inhibition and little band bending imply small $\Delta\mu$ ($\ll 200$ meV). Strong correlations described by the used Hubbard model do not account for the observed depletion inhibition encountered in experiments.

VO_2 electrical properties were found to be insensitive to introduced disorder in experiment [55] and theory [56]. Disorder is unlikely to play a role in the field effect and localization.

Our observations are consistent with field-induced excess charge which is composed of small polarons [57]. When a small polaron forms, an excess carrier induces a lattice deformation which results in a lowering of energy compared to an excess band carrier [see Fig. 4(d)]. The lattice deformation involved is most likely a relaxation of the V dimer see Fig. 4(d)]. Density functional theory simulations indicate a relaxation of the dimer [26] to occur with charging. Because polarons are energetically favorable compared to band carriers and can form at very high density, they will screen the electric field at VO_2's interfaces, resulting in the observed absence of band bending and depletion [see Fig. 4(e)]. A Holstein small polaron model [57] explains the observed excess carrier mobility as shown in Fig. 2. For the adiabatic model, with $\mu = a^2(e/kT)(\omega_0/2\pi)e^{-E_a/kT}$, the fitted parameters are $a^2\hbar\omega_0 = 2$ meV nm, with $\hbar\omega_0 =$ 8–22 meV for hopping distances $a = 0.3$–0.5 nm, and activation energy $E_a = 0.11$ eV. E_a is substantially smaller than the polaron binding energy ($>2E_a$) [57]. Hence, the polaron binding energy is considerable compared to the gap energy. The magnitude of the obtained $\hbar\omega_0$ corresponds to typical optical phonon energies [42], corroborating the presence of small polarons.

The strongly localized carriers screen electric fields and inhibit depletion regions. These space charge regions play a key role in the photovoltaic effect, electroluminescence, lasing, photoconductance, rectification in semiconductor junctions, etc. Their impact can, for example, explain the relatively low VO_2-metal contact resistances [58], Ohmic behavior and absence of rectification in VO_2-metal junctions [58], and the thermal origin of photovoltage [26,59]. The localized carriers can greatly influence the (opto) electronic behavior of strongly correlated materials. These need to be accounted for to identify tailored materials and device concepts with potential large intrinsic field effects or field-induced Mott transitions.

We have measured the field effect of VO_2 in FET structures. Oxygen migration and Joule heating were avoided. The field effect behavior is explained by field-induced excess carriers which are strongly localized, as shown by their low, temperature-activated mobility ($\sim 1 \times 10^{-3}$ cm^2/V s at 300 K, $E_a = 0.11$ eV). A conventional semiconductor field effect as found in some oxides with low mobility [60–63] is found to be absent in VO_2. Depletion behavior is strongly suppressed, as observed in both measurements of subdued field effect modulation of channel current and capacitance. A direct field-induced MIT was not observed with field-induced excess carriers reaching densities of $\sim 5 \times 10^{13}$ cm^{-2}. No signatures of defect-dominated behavior are encountered in admittance spectroscopy of capacitors, channel conductance, and STM. The field effect observations in VO_2 are consistent with the presence of strongly localized carriers behaving as small polarons. Excess charge mobility is in agreement with that of small polarons described by a Holstein model with an extracted

optical phonon frequency of the expected magnitude. The presence of the encountered intrinsic strongly localized carriers has wide-ranging implications for the physics and applications of VO_2 and strongly correlated materials.

The authors acknowledge B. Hughes, K. Roche, L. Gao, C. Lada, J. Van Houdt, M. Heyns, J. P. Locquet, J. Delmotte, L. Krupp, L. Clark, and FWO (K. M.). S. D. and N. S. acknowledge LEAST (Low Energy Systems Technology), one of six SRC STARnet Centers, sponsored by MARCO/DARPA, for financial support.

[1] T. C. Koethe, Z. Hu, M. W. Haverkort, C. Schußler-Langeheine, F. Venturini, N. B. Brookes, O. Tjernberg, W. Reichelt, H. Hsieh, H. J. Lin, C. T. Chen, and L. H. Tjeng, Phys. Rev. Lett. **97**, 116402 (2006).
[2] S. Biermann, A. Poteryaev, A. Lichtenstein, and A. Georges, Phys. Rev. Lett. **94**, 026404 (2005).
[3] J. M. Tomczak, F. Aryasetiawan, and S. Biermann, Phys. Rev. B **78**, 115103 (2008).
[4] J. H. Park, J. M. Coy, T. S. Kasirga, C. Huang, Z. Fei, S. Hunter, and D. H. Cobden, Nature (London) **500**, 431 (2013).
[5] M. M. Qazilbash, A. Tripathi, A. A. Schafgans, B.-J. Kim, H.-T. Kim, Z. Cai, M. V. Holt, J. M. Maser, F. Keilmann, O. G. Shpyrko, and D. N. Basov, Phys. Rev. B **83**, 165108 (2011).
[6] M. K. Liu, M. Wagner, E. Abreu, S. Kittiwatanakul, A. McLeod, Z. Fei, M. Goldflam, S. Dai, M. M. Fogler, J. Lu, S. A. Wolf, R. D. Averitt, and D. N. Basov, Phys. Rev. Lett. **111**, 096602 (2013).
[7] J. Son, B. Jalan, A. P. Kajdos, L. Balents, S. J. Allen, and S. Stemmer, Appl. Phys. Lett. **99**, 192107 (2011).
[8] P. Xiang, S. Asanuma, H. Yamada, H. Sato, and I. Inoue, Adv. Mater. **25**, 2158 (2013).
[9] M. Nakano, K. Shibuya, D. Okuyama, T. Hatano, S. Ono, M. Kawasaki, Y. Iwasa, and Y. Tokura, Nature (London) **487**, 459 (2012).
[10] J. Jeong, N. Aetukuri, T. Graf, T. Schladt, M. Samant, and S. Parkin, Science **339**, 1402 (2013).
[11] A. Zylbersztejn and N. Mott, Phys. Rev. B **11**, 4383 (1975).
[12] J. Goodenough, J. Solid State Chem. **3**, 490 (1971).
[13] M. Liu, H. Hwang, H. Tao, A. Strikwerda, K. Fan, G. Keiser, A. Sternbach, K. West, S. Kittiwatanakul, J. Lu, S. Wolf, F. Omenetto, X. Zhang, K. Nelson, and R. Averitt, Nature (London) **487**, 345 (2012).
[14] J. Pouget, H. Launois, T. Rice, P. Dernier, and A. Gossard, Phys. Rev. B **10**, 1801 (1974).
[15] J. Pouget, H. Launois, J. D'Haenens, P. Merenda, and T. Rice, Phys. Rev. Lett. **35**, 873 (1975).
[16] W. Rosevear and W. Paul, Phys. Rev. B **7**, 2109 (1973).
[17] D. Ruzmetov, G. Gopalakrishnan, C. Ko, V. Narayanamurti, and S. Ramanathan, J. Appl. Phys. **107**, 114516 (2010).
[18] H. T. Kim, B. G. Chae, D. H. Youn, S. L. Maeng, G. Kim, K. Y. Kang, and Y. S. Lim, New J. Phys. **6**, 52 (2004).
[19] M. Belyaev, V. Putrolaynen, A. Velichko, G. Stefanovich, and A. Pergament, Jpn. J. Appl. Phys. **53**, 111102 (2014).
[20] N. Aetukuri, Ph.D. thesis, Stanford University, 2012.
[21] J. C. Duchene, M. Terraillon, M. Pailly, and B. Adam, IEEE Trans. Electron Devices **18**, 1151 (1971).
[22] A. Zimmers, L. Aigouy, M. Mortier, A. Sharoni, S. Wang, K. G. West, J. G. Ramirez, and I. K. Schuller, Phys. Rev. Lett.. **110**, 056601 (2013).
[23] I. P. Radu, B. Govoreanu, S. Mertens, X. Shi, M. Cantoro, M. Schaekers, M. Jurczak, S. D. Gendt, A. Stesmans, J. A. Kittl, M. Heyns, and K. Martens, Nanotechnology **26**, 165202 (2015).
[24] N. Aetukuri, A. Gray, M. Drouard, M. Cossale, H. Durr, M. Samant, and S. Parkin, Nat. Phys. **9**, 661 (2013).
[25] Y. Muraoka and Z. Hiroi, Appl. Phys. Lett. **80**, 583 (2002).
[26] See Supplemental Material at http://link.aps.org/supplemental/10.1103/PhysRevLett.115.196401, which includes Refs. [27–38], for details on thin films, device fabrication, experimental results, and modeling.
[27] E. H. Nicollian and J. R. Brews, *MOS Physics and Technology* (Wiley, New York, 2003).
[28] H. Ueda, T. Kanki, and H. Tanaka, Appl. Phys. Lett. **102**, 153106 (2013).
[29] G. Kresse and J. Furthmuller, Phys. Rev. B **54**, 11169 (1996).
[30] J. Paier, M. Marsman, K. Hummer, G. Kresse, I. C. Gerber, and J. G. Ángyán, J. Chem. Phys. **124**, 154709 (2006); **125**, 249901(E) (2006).
[31] J. Heyd, G. E. Scuseria, and M. Ernzerhof, J. Chem. Phys. **118**, 8207 (2003).
[32] G. Andersson, Acta Chem. Scand. **10**, 623 (1956).
[33] V. Eyert, Ann. Phys. (Leipzig) **11**, 650 (2002).
[34] D. S. Fisher, G. Kotliar, and G. Moeller, Phys Rev. B **52**, 17112 (1995).
[35] P. Werner, A. Comanac, L. de' Medici, M. Troyer, and A. J. Millis, Phys. Rev. Lett. **97**, 076405 (2006).
[36] L. Boehnke, H. Hafermann, M. Ferrero, F. Lechermann, and O. Parcollet, Phys. Rev. B **84**, 075145 (2011).
[37] TRIQS, http://ipht.cea.fr/triqs/.
[38] T. Oka and N. Nagaosa, Phys. Rev. Lett. **95**, 266403 (2005).
[39] K. Martens, N. Aetukuri, J. Jeong, M. Samant, and S. Parkin, Appl. Phys. Lett. **104**, 081918 (2014).
[40] H. Paik, J. A. Moyer, T. Spila, J. W. Tashman, J. A. Mundy, E. Freeman, N. Shukla, J. M. Lapano, R. Engel-Herbert, W. Zander, J. Schubert, D. A. Muller, S. Datta, P. Schiffer, and D. G. Schlom, Appl. Phys. Lett. **107**, 163101 (2015).
[41] A. Delabie, M. Caymax, B. Brijs, D. Brunco, T. Conard, E. Sleeckx, S. V. Elshocht, L. Ragnarsson, S. D. Gendt, and M. Heyns, J. Electrochem. Soc. **153**, F180 (2006).
[42] Landolt-Bornstein Encyclopedia (Springer-Verlag, Berlin, 2013).
[43] N. Tsuda, K. Nasu, A. Fujimori, and K. Siratori, *Electronic Conduction in Oxides* (Springer-Verlag, Berlin, 2000).
[44] R. Srivastava and L. Chase, Phys. Rev. Lett. **27**, 727 (1971).
[45] K. Okazaki, H. Wadati, A. Fujimori, M. Onoda, Y. Muraoka, and Z. Hiroi, Phys. Rev. B **69**, 165104 (2004).
[46] D. Ruzmetov, D. Heiman, V. Narayanamurti, and S. Ramanathan, Phys. Rev. **79**, 153107 (2009).
[47] S. Sze and K. Ng, *Physics of Semiconductor Devices* (John Wiley & Sons, New York, 2007).
[48] S. Blonkowski, Appl. Phys. Lett. **91**, 172903 (2007).
[49] C. Wenger, J. Appl. Phys. **103**, 104103 (2008).
[50] D. Schroder, *Semiconductor Material and Device Characterization* (Wiley, New York, 2006).
[51] K. Martens, C. Chui, B. D. Jaeger, D. Kuzum, M. Meuris, M. Heyns, T. Krishnamohan, K. Saraswat, H. Maes, and G. Groeseneken, IEEE Trans. Electron Devices **55**, 547 (2008).

[52] M. Pollak and T. Geballe, Phys. Rev. **122**, 1742 (1961).
[53] A. Georges, G. Kotliar, W. Krauth, and M. J. Rozenberg, Rev. Mod. Phys. **68**, 13 (1996).
[54] M. Sentef, J. Kunes, P. Werner, and A. P. Kampf, Phys. Rev. B **80**, 155116 (2009).
[55] J. G. Ramirez, T. Saerbeck, S. Wang, J. Trastoy, M. Malnou, J. Lesueur, J.-P. Crocombette, J. E. Villegas, and I. K. Schuller, Phys. Rev. B **91**, 205123 (2015).
[56] C. Weber, D. D. O'Regan, N. D. M. Hine, M. C. Payne, G. Kotliar, and P. B. Littlewood, Phys. Rev. Lett. **108**, 256402 (2012).
[57] T. Holstein, Ann. Phys. (N.Y.) **8**, 343 (1959).
[58] K. Martens, I. Radu, S. Mertens, V. Afanas'ev, J. Kittl, M. Heyns, and M. Jurczak, J. Appl. Phys. **112**, 124501 (2012).
[59] T. Kasirga, D. Sun, J. Park, J. Coy, Z. Fei, X. Xu, and D. Cobden, Nat. Nanotechnol. **7**, 723 (2012).
[60] K. Ueno, I. H. Inoue, T. Yamada, H. Akoh, Y. Tokura, and H. Takagi, Appl. Phys. Lett. **84**, 3726 (2004).
[61] M. Katayama, S. Ikesaka, J. Kuwano, Y. Yamamoto, H. Koinuma, and Y. Matsumoto, Appl. Phys. Lett. **89**, 242103 (2006).
[62] K. Shibuya, T. Ohnishi, T. Uozumi, T. Sato, M. Lippmaa, M. Kawasaki, K. Nakajima, T. Chikyow, and H. Koinuma, Appl. Phys. Lett. **88**, 212116 (2006).
[63] C. H. Ahn, A. Bhattacharya, M. D. Ventra, J. N. Eckstein, C. D. Frisbie, M. E. Gershenson, A. M. Goldman, I. H. Inoue, J. Mannhart, A. J. Millis, A. F. Morpurgo, D. Natelson, and J.-M. Triscone, Rev. Mod. Phys. **78**, 1185 (2006).